Transactions of the Korean Nuclear Society Spring Meeting
Jeju, Korea, May 29-30, 2014

Simulation of Induced Current and Charge Signal Formation on a Position-Sensing CZT Detector with Delay-Line Electrode Scheme

Geehyun Kim[a*], Manhee Jeong[b], Mark D. Hammig[c]
[a]*Department of Nuclear Engineering, Sejong University, Seoul, South Korea*
[b]*Korea Atomic Energy Research Institute (KAERI), Daejeon, South Korea*
[c]*Dept. of Nuclear Eng. and Radiological Sci., The University of Michigan, Ann Arbor, MI 48109, USA*
[*]*Corresponding author: gkim01@sejong.ac.kr*

1. Introduction

In this research, we performed analytic simulations on the signal formation of the position-sensitive nuclear radiation detector with the delay-line electrode scheme, by investigating both induced current and charge signals created by the drifting charge carriers. The position-sensing scheme using serpentine delay-lines patterned on the semiconductor detector surface has been studied as a means of simplifying the readout electronics and reducing the power requirements of the nuclear radiation detection system [1]-[3]. We simulated the propagation of the induced current signal along the delay-line pattern simultaneously with the drift motion of the charge carriers attributed by the electric field configuration within the semiconductor crystal, which is also calculated with a high frequency structure simulator software. The calculation result was compared with the position-specific signals obtained from a low-noise silicon detector.

2. Methods and Results

2.1 Calculation Methods

For the calculation of the induced current and charge signals, we started from calculating weighting potential configuration of the detector material based on the Shockley-Ramo Theorem by solving Poisson's equation using an electromagnetic simulation software, called MAXWELL® 12.0. Fig. 1a and 1b show an example of the simulation geometry and the weighting potential result calculated for a pixel bin (a sub-area of the line segment), assuming 1 V applied on the pixel of our interest, whereas setting the rest of them as 0V. The top electrode of the detector was composed of 5 turns of the line segment, each consists of 50 pixel bins.

Drifting tracks of the charge carriers determined by the electric field vectors were simulated assuming a typical 1000 V bias applied to the 5 mm-thick CZT detector, the simulation was performed for various interaction positions; that is, for different spatial distributions of electric-hole pairs. When the electric field vectors were calculated, the entire pattern was assumed to be at the same potential as well as the guard rings to configure a constant and uniform electric field created under the pattern area. Induced current, a certain pixel bin feels, can be calculated from the weighting field and the drift motion simulation of the charge carrier. Induced current at each time step was calculated by taking the dot product of the drift velocity component and the weighting electric field, and the induced current signal is transmitted through the delay-lines from the current bin to the next bin as illustrated in Fig. 1c. Since the simulation still takes a discretized approach, note that there is always limitation in showing the continuous distribution and propagation of the signal.

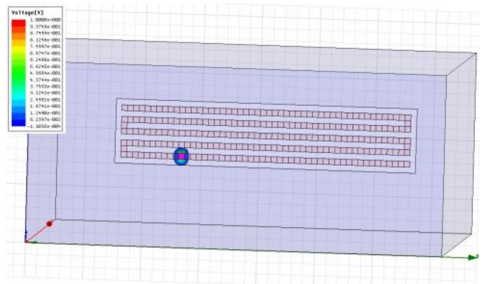

(a)

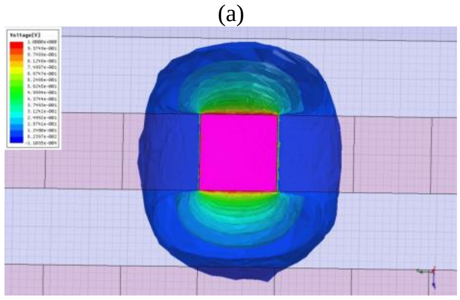

(b)

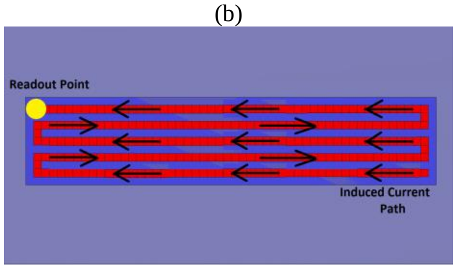

(c)

Fig. 1. MAXWELL simulation configuration for 5-turn meandering electrode pattern geometry on a 5 mm-thick CZT crystal and the weighting potential calculated for a certain pixel bin. (b) Detailed view of the weighting potential around the pixel bin of interest. Weighting potential was calculated by solving Poisson's equation for the entire detector volume, assuming 1 V applied on the pixel of interest and the rest of them were set to 0 V. (c) Schematic illustration of propagation of the induced current in one direction for one readout point.

2.2 Signal Formation from the Multiple Strip

We simulated the signal formation in both ways – by calculating induced current and induced charge – from the multiple meandering delay-line strip by tracking the motion of drifting charge carriers created by the incident radiation interaction. Fig. 2 shows an example of the induced current and charge calculation result.

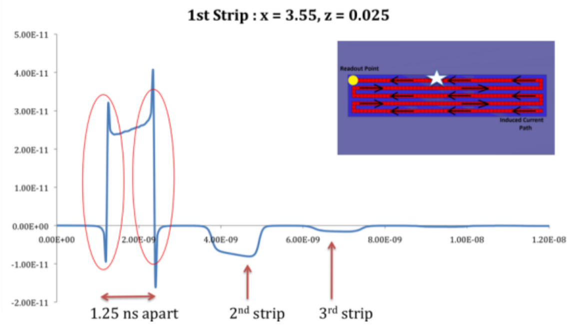

(a)

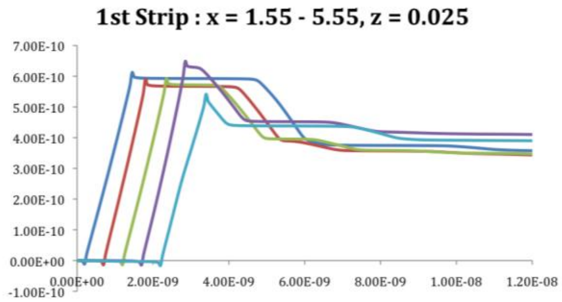

(b)

Fig. 2. A simulation result of (a) current and (b) charge induced on the pixel bins as charge carriers are collected as the time propagates. The induced charge was calculated by integrating induced current for various x-positions in a strip.

2.3 Induced Charge and Current from the Planar Side

Whereas the weighting potential of the pattern gives a small pixel effect in the signal formation of the pattern signal, the weighting potential in the other electrode side develops uniformly and linearly from the pattern side to the un-patterned (cathode) side. Fig. 3 shows the result calculated for the planar-side of the detector.

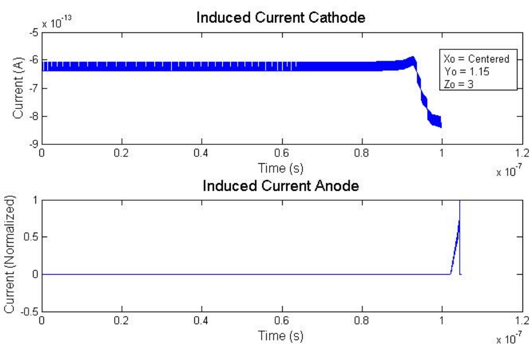

(a)

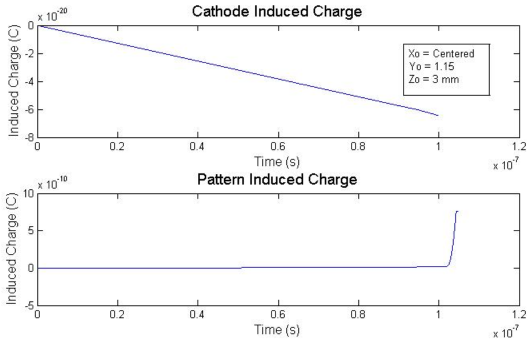

(b)

Fig. 3. Induced (a) current and (b) charge signal on both sides of the detector from a single charge carrier generated at deep position (3 mm) underneath the center position of the pattern.

2.4 Comparison with Experimental Results

The result was confirmed by the experimental results obtained from a low-noise p-i-n diode type silicon detector with delay-line electrode pattern on the high-resistivity silicon wafers, as shown in Fig. 4.

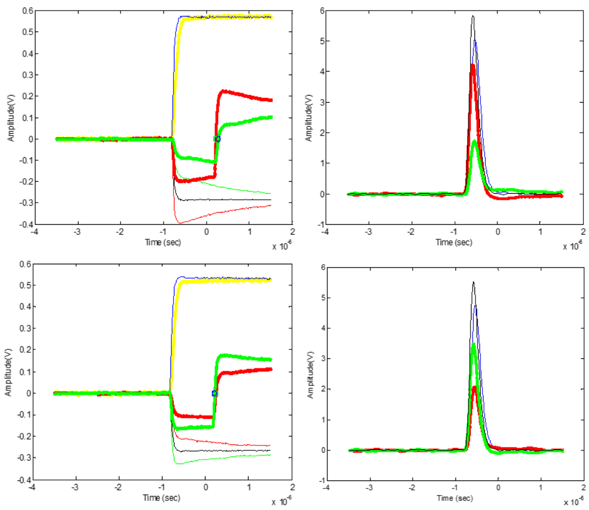

Fig. 4. Signals acquired for the interactions happened at one line-segment of the pattern end (top) and the other (bottom).

3. Conclusions

In this research we simulated the formation of the induced charge and the induced current signal based on the weighting-potential method by tracking the drifting motion of charge carriers within the CZT crystal. The result was compared with the position-sensitive signal obtained from a low-noise silicon detector made from a high-resistivity silicon wafer.

REFERENCES

[1] G. Kim, J. Karbowski, and M.D. Hammig, *Nucl. Instr. and Meth.* **A** 652, pp. 439 (2011).
[2] M. D. Hammig, M. Jeong, D.K. Wehe, and S. Ramadoss, *IEEE NSS-MIC Conf. Rec.*, p 2493 (2008).
[3] M. Jeong, M.D. Hammig and S. Ramadoss, *IEEE NSS-MIC Conf. Rec.*, p 1666-1673 (2009).